

# Calculations of Electron Inelastic Mean Free Paths.

## V. Data for 14 Organic Compounds over the 50–2000 eV Range

**S. Tanuma**

Analysis Research Center, Nippon Mining Company Ltd., 3-17-35 Niizo-Minami, Toda, Saitama 335, Japan

**C. J. Powell and D. R. Penn**

National Institute of Standards and Technology, Gaithersburg, MD 20899, USA

We report calculations of electron inelastic mean free paths (IMFPs) of 50–2000 eV electrons for a group of 14 organic compounds: 26-*n*-paraffin, adenine,  $\beta$ -carotene, bovine plasma albumin, deoxyribonucleic acid, diphenyl-hexatriene, guanine, kapton, polyacetylene, poly(butene-1-sulfone), polyethylene, polymethylmethacrylate, polystyrene and poly(2-vinylpyridine). The computed IMFPs for these compounds showed greater similarities in magnitude and in the dependences on electron energy than was found in our previous calculations for groups of elements and inorganic compounds (Papers II and III in this series). Comparison of the IMFPs for the organic compounds with values obtained from our predictive IMFP formula TPP-2 showed systematic differences of  $\sim 40\%$ . These differences are due to the extrapolation of TPP-2 from the regime of mainly high-density elements (from which it had been developed and tested) to the low-density materials such as the organic compounds. We analyzed the IMFP data for the groups of elements and organic compounds together and derived a modified empirical expression for one of the parameters in our predictive IMFP equation. The modified equation, denoted TPP-2M, is believed to be satisfactory for estimating IMFPs in elements, inorganic compounds and organic compounds.

### INTRODUCTION

In previous papers of this series<sup>1–4</sup> we have described an algorithm for the calculation of electron inelastic mean free paths (IMFPs) in solids,<sup>1</sup> used this algorithm for the calculation of IMFPs for 50–2000 eV electrons in a group of 27 elements<sup>2</sup> and a group of 15 inorganic compounds,<sup>3</sup> and presented an evaluation of the calculated IMFPs.<sup>4</sup> We fitted the calculated IMFPs for the group of elements to a modified form of the Bethe equation<sup>5</sup> for inelastic electron scattering in matter and found that the four parameters in this equation could be related empirically to several material parameters (atomic weight, density, number of valence electrons per atom and bandgap energy).<sup>2</sup> The resulting equation, designated TPP-2, gave IMFP values for the 27 elements that differed from those initially calculated by 13% root mean square (RMS). The TPP-2 formula could then be used to estimate IMFPs for other materials. An assessment of the reliability of the TPP-2 formula was presented in Paper IV.<sup>4</sup>

We report here IMFP calculations for 50–2000 eV electrons in 14 organic compounds: 26-*n*-paraffin, adenine,  $\beta$ -carotene, bovine plasma albumin (BPA), deoxyribonucleic acid (DNA), diphenyl-hexatriene, guanine, kapton, polyacetylene, poly(butene-1-sulfone), polyethylene, polymethylmethacrylate (PMMA), polystyrene and poly(2-vinylpyridine). These 14 compounds were selected because the optical data needed for the IMFP calculations were available.

We found that the calculated IMFPs for each of the 14 organic compounds were  $\sim 40\%$  larger than values expected from the TPP-2 formula. On further examination of the sets of IMFP data for the groups of elements and organic compounds, we concluded that the TPP-2 formula was based largely on data for high-density solids (mainly transition metals) while the organic compounds are of much lower density. We present here an analysis of the IMFP data for the combined groups of elements and organic compounds from which we have derived a modified expression for one of the parameters in TPP-2. The new predictive IMFP equation is designated TPP-2M.

### INELASTIC MEAN FREE PATH CALCULATION

Our method for the IMFP calculation has been described previously.<sup>1,2</sup> We make use of the Penn<sup>6</sup> algorithm, which is expected to give useful results for electron energies above 50 eV.<sup>4</sup> We have, in addition, calculated IMFPs for electron energies between 10 and 40 eV and display these results in the figures presented below to show the IMFP trends *vs.* electron energy more completely; these results should be considered only as rough estimates. The IMFP values were calculated using Eqn (14) of Ref. 1 for electron energies between 10 and 700 eV and Eqn (16) of Ref. 1 was used for energies between 800 and 2000 eV. All energies are

**Table 1. Sources of optical data used in the IMFP calculations**

Compound	Photon energy range (eV)	Source of data
26- <i>n</i> -Paraffin	6–40	Ref. 7
	50–30 000	Ref. 8
Adenine	4–55	Ref. 9
	58–30 000	Ref. 8
$\beta$ -Carotene	0.7–44	Ref. 7
	50–30 000	Ref. 8
BPA	4–82	Ref. 10
DNA	4.2–82	Ref. 11
Diphenyl-hexatriene	0.7–42	Ref. 7
	50–30 000	Ref. 8
Guanine	2.8–49	Ref. 12
	50–30 000	Ref. 8
Kapton	2.0–65	Ref. 13
	68–30 000	Ref. 8
Polyacetylene	1–59	Ref. 14
	61–30 000	Ref. 8
Poly(butene-1-sulfone)	5.6–39	Ref. 15
	50–9886	Ref. 8
Polyethylene	5–60	Ref. 16
	70–9886	Ref. 8
PMMA	5–70	Ref. 17
	72–30 000	Ref. 8
Polystyrene	4–64	Ref. 18
	65–30 000	Ref. 8
Poly(2-vinylpyridine)	4–33	Ref. 19
	35–30 000	Ref. 8

expressed with respect to the Fermi level which, for insulators, is assumed to be located midway between the valence band maximum and the conduction band minimum.

The IMFPs were calculated using values of the electron energy loss function  $\text{Im}[-1/\epsilon(\omega)]$ , where  $\epsilon(\omega)$  is the complex dielectric constant for the material of interest as a function of photon energy  $\hbar\omega$ . Values of the energy loss function were calculated from the sources of optical data listed in Table 1.<sup>7–19</sup>

Figure 1 shows the energy loss function for polystyrene as an example. The dominant feature is the peak

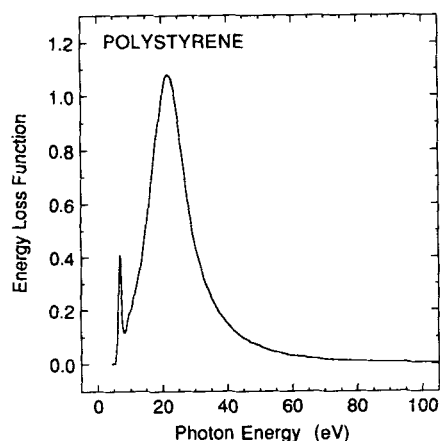


**Figure 1.** Plot of the electron energy loss function  $\text{Im}[-1/\epsilon(\omega)]$  for polystyrene as a function of photon energy  $\hbar\omega$ , as calculated from optical data (Table 1).

located at a photon energy of  $\sim 22$  eV; the other organic compounds considered here show a similar peak at energies between 20 and 25 eV. There is a weaker feature in Fig. 1 located at  $\sim 7$  eV; some of the other organic solids do not show any obvious structure in this region, while others show up to three weak peaks.

As indicated by Fig. 1, the most significant contributions to the inelastic scattering cross-section (and thus to the IMFP) occur for photon energies between 5 and 50 eV. Experimental optical data exist for most of the range (Table 1), but it was necessary to make use of atomic photoabsorption data<sup>8</sup> for extrapolations to photon energies beyond the experimental data range now available. These extrapolations are not considered a serious source of error because  $\epsilon(\omega)$  for photon energies greater than  $\sim 50$  eV is mainly determined by atomic properties except in the vicinity of core-electron excitation thresholds. The latter differences are unimportant in the IMFP calculation because an integration of the energy loss function is made over energy.<sup>1</sup> We were not, however, able to make extrapolations for BPA and DNA on account of uncertainty over the chemical formulae for these compounds.

We have evaluated the accuracy of our sets of  $\text{Im}[-1/\epsilon(\omega)]$  data using two useful sum rules. These sum rules are the oscillator strength rule (or f-sum rule) and a limiting form of the Kramers–Kronig integral (or KK-sum rule). The f-sum can be evaluated as the total effective number of electrons per molecule  $Z_{\text{eff}}$  contributing to the inelastic scattering<sup>3</sup>

$$Z_{\text{eff}} = (2/\pi\hbar^2\Omega_p^2) \int_0^{\Delta E_{\text{max}}} \Delta E \text{Im}[-1/\epsilon(\Delta E)] d(\Delta E) \quad (1)$$

where  $\Delta E = \hbar\omega$ ,  $\Omega_p = (4\pi n_a e^2/m)^{1/2}$ ,  $n_a = N_a \rho/M$  is the density of molecules,  $N_a$  is Avogadro's number,  $\rho$  is the bulk density and  $M$  is the molecular weight. When the upper limit in Eqn (1) is equal to infinity,  $Z_{\text{eff}}$  should be equal to  $Z$ , the total number of electrons per molecule. The KK-sum can be expressed as<sup>3</sup>

$$P_{\text{eff}} = (2/\pi) \int_0^{\Delta E_{\text{max}}} \Delta E^{-1} \times \text{Im}[-1/\epsilon(\Delta E)] d(\Delta E) + n^{-2}(0) \quad (2)$$

where  $n(0)$  is the limiting value of the refractive index at frequencies below those where absorption maxima are observed. In the limit  $\Delta E_{\text{max}} \rightarrow \infty$ ,  $P_{\text{eff}} \rightarrow 1$ . Additional information on the use of these sum rules is presented elsewhere.<sup>20</sup>

Evaluations of Eqns (1) and (2) are given in Figs 2 and 3 for polystyrene as an example. The plot of the f-sum integral in Fig. 2 as a function of  $\Delta E_{\text{max}}$  shows two regions corresponding to the excitation of valence electrons and carbon K-shell electrons. The limiting value of  $Z_{\text{eff}}$  is 54.5 rather than the expected value  $Z = 56$ , an error of  $-2.6\%$ . The plot of the KK-sum integral in Fig. 3 shows an initial value of  $P_{\text{eff}} = 0.418$  [associated with the second term in Eqn (2)] and a limiting value of  $P_{\text{eff}} = 1.009$  for large  $\Delta E_{\text{max}}$  rather than the expected value of unity, an error of  $0.9\%$ . It is interesting to note that  $P_{\text{eff}}$  in Fig. 3 essentially reaches its saturation value for  $\Delta E_{\text{max}} \sim 100$  eV; i.e., there is no significant contribution to the integral in Eqn (2) from K-shell electrons.<sup>20</sup>

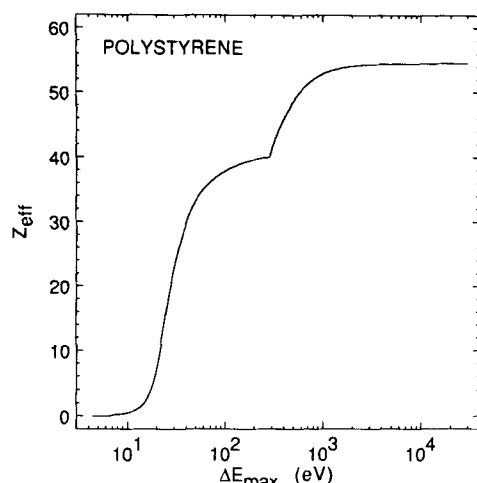


**Figure 2.** Plot of  $Z_{\text{eff}}$  determined from Eqn (1) for polystyrene as a function of the upper limit in the integration  $\Delta E_{\text{max}}$ .

Table 2 lists the errors in the f-sum and KK-sum rules for this group of organic compounds. As noted earlier, it was not possible to evaluate the f-sum for BPA and DNA because we could not make a reliable estimate of the optical constants for these compounds at photon energies greater than 82 eV; as indicated by the example of Fig. 3, it was nevertheless possible to obtain a sufficiently reliable measure of the KK-sum for these two compounds because  $P_{\text{eff}}$  is within 1% of its maximum value when  $\Delta E_{\text{max}} > 52$  eV. The average root-mean-square (RMS) error for the data evaluations based on the f-sum rule is  $\sim 7\%$  while that for the KK-sum rule is  $\sim 2\%$ . These RMS errors are considered acceptably small for the IMFP calculation.<sup>4</sup>

Knowledge of the Fermi energy is required for the IMFP calculation.<sup>1</sup> We have chosen arbitrarily a value of  $E_F = 15$  eV for the calculations reported here because reasonable variation of this parameter did not significantly affect the IMFP values found for the inorganic compounds.<sup>3</sup>

We expect our IMFP results to be useful for electron energies greater than  $\sim 50$  eV.<sup>4</sup> The uncertainties in the IMFPs for energies between 50 and 200 eV will be greater than those for higher energies. Further informa-

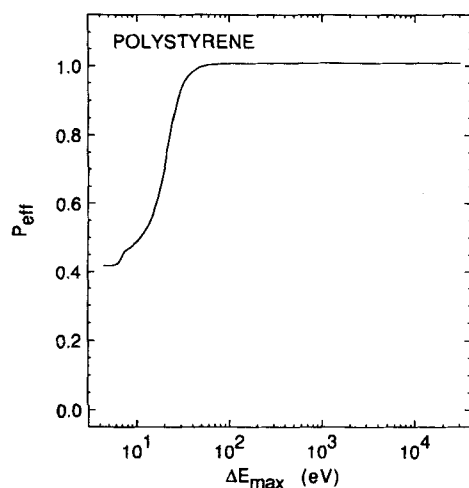


**Figure 3.** Plot of  $P_{\text{eff}}$  determined from Eqn (2) for polystyrene as a function of the upper limit in the integration  $\Delta E_{\text{max}}$ .

**Table 2.** Errors in the f-sum [Eqn (1)] and the KK-sum [Eqn (2)] rules for the indicated compounds<sup>a</sup>

Compound	Error in f-sum rule (%)	Error in KK-sum rule (%)
26- <i>n</i> -Paraffin	-16	2
Adenine	-3	5
$\beta$ -Carotene	-7	3
BPA	<sup>b</sup>	-2 <sup>c</sup>
DNA	<sup>b</sup>	-2 <sup>c</sup>
Diphenyl-hexatriene	-2	3
Guanine	-2	2 <sup>c</sup>
Kapton	7	-1
Polyacetylene	12	-2
Poly(butene-1-sulfone)	-3	1 <sup>c</sup>
Polyethylene	0	1
PMMA	-7	-4 <sup>c</sup>
Polystyrene	-3	1 <sup>c</sup>
Poly(2-vinylpyridine)	0 <sup>d</sup>	-1

<sup>a</sup> The sum rules have been evaluated using values of  $\Delta E_{\text{max}}$  equal to the highest photon energy for the data listed in Table 1. A minus (plus) indicates that the values of  $Z_{\text{eff}}$  and  $P_{\text{eff}}$  were less than (greater than) the expected values.

<sup>b</sup> It was not possible to obtain a reliable value of the f-sum for BPA and DNA (see text).

<sup>c</sup> We used values of the refractive index at photon energies of 2, 2, 2.2, 1, 3 and 0.6 eV for BPA, DNA, guanine, poly(butene-1-sulfone), PMMA and polystyrene, respectively, in the evaluation of  $P_{\text{eff}}$  from Eqn (2).

<sup>d</sup> Based on the deduced density shown in Table 5.

tion on uncertainties of the calculated IMFPs is given in Paper IV.<sup>4</sup>

## IMFP RESULTS

Table 3 shows IMFP values calculated from the optical data for 50–2000 eV electrons in the 14 organic compounds. Plots of IMFP vs. electron energy are shown in Figs 4–8 for 26-*n*-paraffin, DNA, polyethylene, PMMA and polystyrene as examples of our results. The insets in each figure show IMFP values at low energies ( $< 200$  eV) on an expanded energy scale; as noted earlier, the data for energies between 10 and 40 eV are presented to indicate trends and should only be regarded as estimates.

Figure 9 is a summary plot showing the calculated IMFPs for the group of organic compounds vs. electron energy over the 50–2000 eV range. The calculated IMFPs for these compounds show several similarities. First, the results for different compounds at a given energy are of similar magnitude; for instance, the ratio of the maximum IMFP at one energy to the minimum IMFP varies from 1.38 to 1.47. Second, the IMFP dependence on energy is very similar from compound to compound. Finally, the IMFP–energy curve all exhibit minima at energies of  $\sim 60$ –70 eV.

As a group, the organic compounds show much greater homogeneity in their IMFP properties than the groups of elements<sup>2</sup> and inorganic compounds<sup>3</sup> analyzed previously. The similarity in IMFP results for the organic compounds is not considered surprising because they have very similar densities (see Table 5

**Table 3. Inelastic mean free paths as a function of energy for 14 organic compounds**

Electron energy (eV)	Inelastic mean free path (Å)													
	26-n-Paraffin	Adenine	$\beta$ -Carotene	BPA	DNA	Diphenyl-hexatriene	Guanine	Kapton	Poly-acetylene	Poly(butene-1-sulfone)	Poly-ethylene	PMMA	Poly-styrene	Poly(2-vinylpyridine)
50	7.0	6.4	6.4	7.3	7.3	6.4	6.2	7.0	5.3	7.1	6.9	7.8	6.9	6.9
100	7.6	6.6	7.0	7.2	7.3	7.0	6.2	6.8	5.7	7.2	7.2	7.9	7.3	7.3
150	9.2	7.8	8.5	8.5	8.5	8.4	7.2	7.9	6.8	8.5	8.6	9.3	8.7	8.7
200	10.9	9.2	10.0	9.9	9.8	9.9	8.4	9.2	7.9	9.9	10.1	10.8	10.2	10.3
300	14.1	11.8	13.0	12.7	12.6	12.9	10.8	11.7	10.2	12.7	13.0	13.9	13.2	13.3
400	17.2	14.4	15.9	15.4	15.4	15.8	13.1	14.2	12.5	15.4	15.9	16.9	16.1	16.2
500	20.3	16.8	18.7	18.1	18.1	18.6	15.3	16.7	14.7	18.1	18.7	19.8	18.9	19.0
600	23.2	19.2	21.4	20.7	20.7	21.3	17.5	19.0	16.9	20.7	21.4	22.7	21.6	21.8
700	26.1	21.6	24.1	23.3	23.2	24.0	19.6	21.4	18.9	23.2	24.0	25.4	24.3	24.5
800	29.2	24.1	26.9	25.8	25.9	26.7	21.8	23.7	21.1	25.8	26.8	28.3	27.1	27.3
900	32.0	26.4	29.4	28.3	28.3	29.3	23.9	26.0	23.1	28.2	29.3	31.0	29.7	29.9
1000	34.7	28.6	32.0	30.8	30.8	31.8	25.9	28.2	25.1	30.6	31.8	33.7	32.2	32.5
1100	37.4	30.9	34.5	33.2	33.2	34.3	27.9	30.3	27.0	33.0	34.3	36.3	34.7	35.0
1200	40.1	33.1	37.0	35.6	35.6	36.8	29.9	32.5	29.0	35.3	36.8	38.8	37.2	37.5
1300	42.8	35.2	39.4	37.9	37.9	39.2	31.9	34.6	30.9	37.6	39.2	41.4	39.6	40.0
1400	45.4	37.4	41.9	40.2	40.3	41.7	33.8	36.7	32.8	39.9	41.6	43.9	42.1	42.4
1500	48.0	39.5	44.3	42.5	42.6	44.0	35.7	38.8	34.6	42.2	44.0	46.4	44.5	44.9
1600	50.6	41.6	46.6	44.8	44.9	46.4	37.6	40.9	36.5	44.4	46.3	48.9	46.9	47.3
1700	53.1	43.7	49.0	47.1	47.1	48.8	39.5	42.9	38.3	46.6	48.7	51.3	49.2	49.7
1800	55.7	45.8	51.3	49.4	49.4	51.1	41.4	44.9	40.2	48.8	51.0	53.8	51.6	52.0
1900	58.2	47.8	53.7	51.6	51.6	53.4	43.3	47.0	42.0	51.0	53.3	56.2	53.9	54.4
2000	60.7	49.9	56.0	53.8	53.8	55.7	45.1	49.0	43.8	53.2	55.6	58.6	56.2	56.7

below) and the energy loss functions for each material are very similar to that for polystyrene in Fig. 1.

We analyzed the IMFP data for each organic compound in the same way as for the elements<sup>2</sup> and inorganic compounds.<sup>3</sup> We fitted IMFP values for each material to a modified form of the Bethe equation<sup>5</sup> for inelastic electron scattering in matter; the modifications

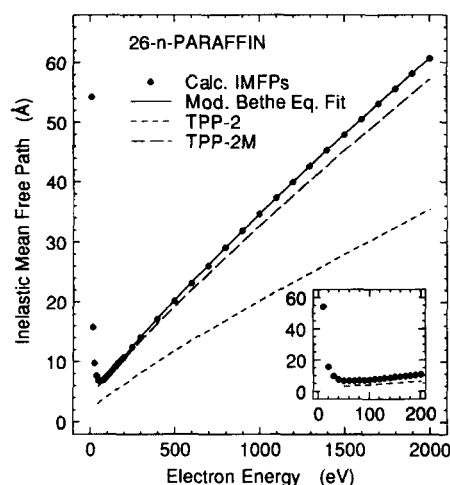


**Figure 4.** Inelastic mean free path values (solid circles) calculated for 26-n-paraffin as a function of electron energy. The IMFP values are shown for 10–40 eV electrons to illustrate trends but these results are not considered to be reliable (see text). The solid line is a fit to the IMFP values with the modified Bethe equation [Eqn (3)]; values of the parameters found in the fit are given in Table 4. The short-dashed line shows IMFP values calculated from the predictive formula TPP-2 [Eqns (3) and (4)], where values of the four parameters in Eqn (3) were calculated using Eqn (4) and property data for 26-n-paraffin as listed in Table 5. The long-dashed line shows IMFP values calculated from the modified predictive formula TPP-2M [Eqns (3), (4b), (4c), (4d), (4e) and (8)]. The inset shows the low-energy region on an expanded energy scale.

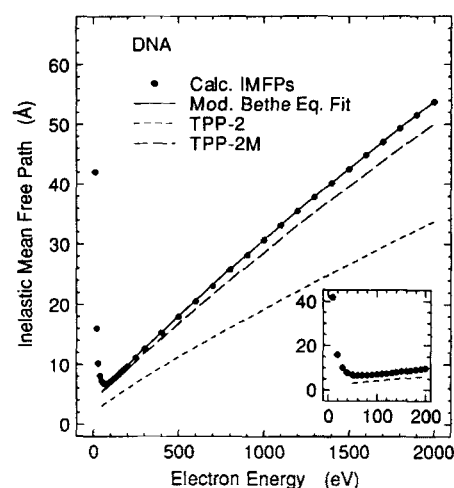


**Figure 5.** Inelastic mean free path results for DNA as a function of electron energy; see caption to Fig. 4.

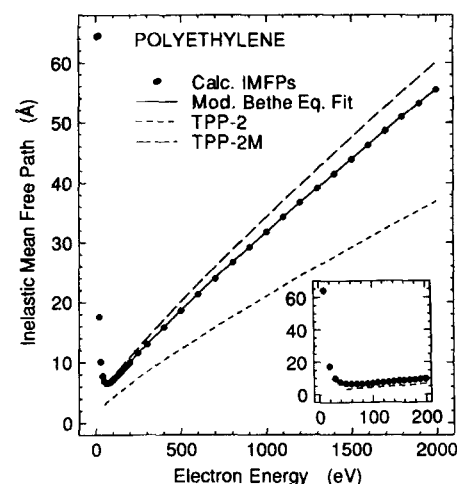


**Figure 6.** Inelastic mean free path results for polyethylene as a function of electron energy; see caption to Fig. 4.

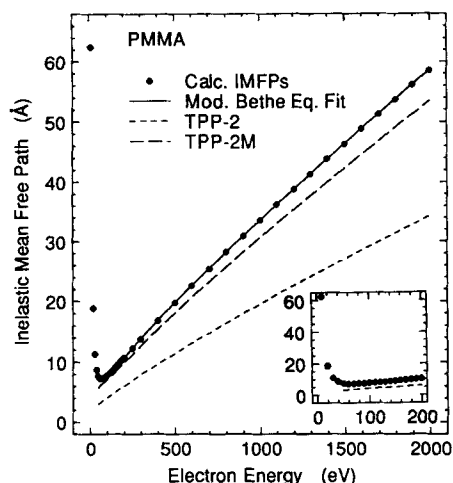


**Figure 7.** Inelastic mean free path results for PMMA as a function of electron energy; see caption to Fig. 4.

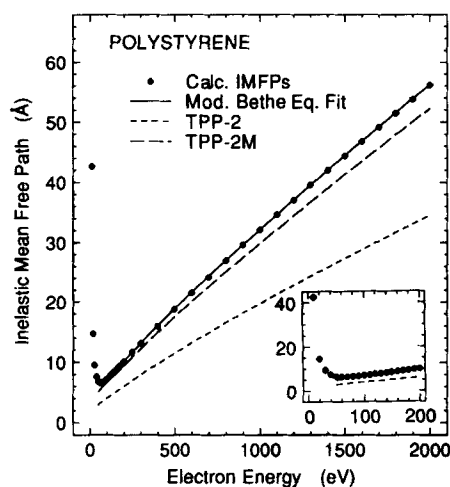


**Figure 8.** Inelastic mean free path results for polystyrene as a function of electron energy; see caption to Fig. 4.

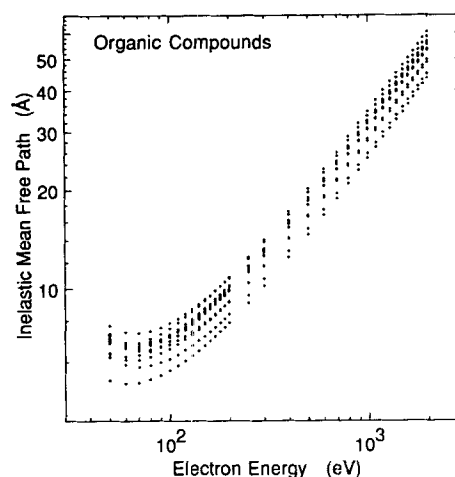


**Figure 9.** Summary plot of calculated IMFPs for the group of organic compounds (Table 3) as a function of electron energy.

were as suggested by Inokuti<sup>21</sup> and Ashley<sup>22</sup> to describe the IMFP dependence on energy for energies less than 200 eV.

The modified Bethe equation is

$$\lambda = E / \{ E_p^2 [\beta \ln(\gamma E) - (C/E) + (D/E^2)] \} \quad (3)$$

where  $\lambda$  is the IMFP (in Å),  $E$  is the electron energy (in eV),  $E_p = 28.8(N_v \rho / M)^{1/2}$  is the free-electron plasmon energy (in eV),  $\rho$  is the density (in g cm<sup>-3</sup>),  $N_v$  is the number of valence electrons per atom (for elements) or molecule (for compounds) and  $M$  is the atomic or molecular weight;  $\beta$ ,  $\gamma$ ,  $C$  and  $D$  are parameters.

The solid lines in Figs 4–8 show fits in Eqn (3) to the IMFP results (Table 3) over the 50–2000 eV range. Values of the parameters  $\beta$ ,  $\gamma$ ,  $C$  and  $D$  for each compound are listed in Table 4, and values of the material parameters used in our analysis are given in Table 5; in many instances, we have used material parameters listed by Ashley.<sup>23</sup>

**Table 4.** Values of the parameters  $\beta$ ,  $\gamma$ ,  $C$  and  $D$  found in the fits of Eqn (3) to the IMFP data for each compound together with values of  $\beta_{\text{opt}}$  calculated from Eqn (6) of Paper III<sup>3</sup>

Compound	$\beta_{\text{opt}}$ (eV <sup>-1</sup> Å <sup>-1</sup> )	$\beta$ (eV <sup>-1</sup> Å <sup>-1</sup> )	$\gamma$ (eV <sup>-1</sup> )	$C$ (Å <sup>-1</sup> )	$D$ (eV Å <sup>-1</sup> )
26- <i>n</i> -Paraffin	0.0156	0.0160	0.175	1.01	14.9
Adenine	0.0165	0.0169	0.159	1.24	21.9
$\beta$ -Carotene	0.0179	0.0184	0.181	1.16	15.9
BPA	0.0171	0.0171	0.195	1.61	30.0
DNA	0.0146	0.0162	0.161	1.25	20.5
Diphenyl-hexatriene	0.0192	0.0198	0.180	1.27	17.9
Guanine	0.0157	0.0161	0.153	1.28	23.8
Kapton	0.0174	0.0177	0.150	1.48	28.3
Polyacetylene	0.0213	0.0216	0.185	1.71	30.7
Poly(butene-1-sulfone)	0.0161	0.0168	0.136	1.10	18.3
Polyethylene	0.0184	0.0188	0.169	1.33	20.7
PMMA	0.0149	0.0152	0.155	1.15	21.0
Polystyrene	0.0179	0.0184	0.168	1.28	20.5
Poly(2-vinylpyridine)	0.0187	0.0191	0.172	1.32	20.3

**Table 5.** Values of the material parameters used in the analysis of the IMFP data for the indicated compounds

Compound	$\rho$ (g cm <sup>-3</sup> )	$M$	$N_v$	$E_p$ (eV)	$E_g$ (eV)
26- <i>n</i> -Paraffin	0.99 <sup>a</sup>	366.7	158	18.8	6
Adenine	1.35	135.1	50	20.4	3.8
$\beta$ -Carotene	0.993 <sup>a</sup>	536.9	216	18.2	0 <sup>b</sup>
BPA	1.14	66 000	25 700	19.2	5.5
DNA	1.35	664	238	20.0	4
Diphenyl-hexatriene	0.986 <sup>a</sup>	232.3	88	17.6	0 <sup>b</sup>
Guanine	1.58	151.1	56	22.0	2.5
Kapton	1.36	382.3	138	20.2	3.5
Polyacetylene <sup>c</sup>	1.13	26.0	10	19.0	1.2
Poly(butene-1-sulfone) <sup>c</sup>	1.39	120.2	42	20.1	6
Polyethylene <sup>c</sup>	0.93	28.1	12	18.2	7
PMMA <sup>c</sup>	1.19	100.1	40	19.9	5
Polystyrene <sup>c</sup>	1.05	104.2	40	18.3	4.5
Poly(2-vinylpyridine) <sup>c</sup>	1.01 <sup>d</sup>	105.1	40	17.9	4

<sup>a</sup> Deduced from  $E_p$  value quoted by Ashley (Ref. 23).<sup>b</sup> Bandgap energy not known but believed to be small (Ref. 23).<sup>c</sup> Values of  $M$  and  $N_v$  are for the monomer.<sup>d</sup> Estimated by assuming that the f-sum rule [Eqn (1)] was satisfied (i.e.  $Z_{\text{eff}} = Z$ ).

From an analysis of calculated IMFPs for 27 elements,<sup>2</sup> we found that the four parameters in Eqn (3) could be related empirically to other material property data, as follows

$$\beta = -0.0216 + 0.944/(E_p^2 + E_g^2)^{1/2} + 7.39 \times 10^{-4} \rho \quad (4a)$$

$$\gamma = 0.191 \rho^{-0.50} \quad (4b)$$

$$C = 1.97 - 0.91U \quad (4c)$$

$$D = 53.4 - 20.8U \quad (4d)$$

$$U = N_v \rho / M = E_p^2 / 829.4 \quad (4e)$$

where  $E_g$  is the bandgap energy (in eV) for non-conductors. Equations (3) and (4) represent our TPP-2 formula for predicting IMFPs in materials.

The short-dashed lines in Figs 4–8 show IMFP values calculated from TPP-2 and the material property data in Table 5. For these compounds (and for the others not shown), the TPP-2 formula gives IMFP values  $\sim 40\%$  lower than those calculated from the optical data. This discrepancy is due to the fact that the TPP-2 formula was developed from an analysis of calculated IMFPs for the group of 27 elements. This group contained many transition metals of generally high density. As a result, the TPP-2 formula is here being extrapolated from the range of densities for which it was developed to a range of much lower densities for which it has not previously been tested.

As a check on our analysis, we have made independent determinations of  $\beta$  valid for 'high' electron energies. These values of  $\beta$ , denoted  $\beta_{\text{opt}}$ , represent the slopes of the Fano plots (in which  $E/\lambda$  is plotted versus  $\ln E$ ) in the so-called asymptotic Bethe region.<sup>24</sup> We have calculated values of  $\beta_{\text{opt}}$  for the organic compounds from an integral of the energy loss function [Eqn (6) of Paper III<sup>3</sup>] with upper limits corresponding to the maximum photon energies for the data sources in

Table 1. Table 4 shows our values of  $\beta_{\text{opt}}$ , which are less than those of  $\beta$  by amounts varying from 0–10%. It is expected<sup>24</sup> that the slopes of the Fano plots for the 50–2000 eV range of electron energies (given by  $\beta$ ) should exceed the asymptotic slopes  $\beta_{\text{opt}}$ ; as a result, Eqns (3) and (4) should not be used for energies greater than 2000 eV.

#### Development of the modified predictive formula TPP-2M

The density of the solid affects the magnitude of the computed IMFP from TPP-2 mainly through the expression for  $\beta$  [Eqn (4a)]. We have derived a modified expression for  $\beta$  based on an analysis of the calculated IMFPs for the group of 27 elements<sup>2</sup> and the present group of 14 organic compounds. The IMFPs for the group of 15 inorganic compounds<sup>3</sup> have been excluded from this analysis because the optical data on which their IMFPs are based are much less reliable than for the other two groups of materials; we do, however, show data derived from the group of inorganic materials to indicate the general similarities for all three groups of materials.

Our data analysis follows that given in Paper II.<sup>2</sup> Figure 10 is a plot of the values of  $\beta$  found in the fits of Eqn (3) to the calculated IMFPs vs.  $(E_p^2 + E_g^2)^{-1/2}$  for the groups of elements, organic compounds and inorganic compounds. The solid line in Fig. 10 is a plot of Eqn (4a) with  $\rho = 10 \text{ g cm}^{-3}$ . Figure 10 shows an approximately linear relationship but, as before, we find deviations that depend on density. Figure 11 is a plot of the residual  $\beta_r$  defined by

$$\beta_r = \beta - 0.944(E_p^2 + E_g^2)^{-1/2} \quad (5)$$

as a function of density. The dashed line in Fig. 11 is the empirical linear dependence of  $\beta_r$  that we developed previously from the analysis of the elemental IMFPs;<sup>2</sup>

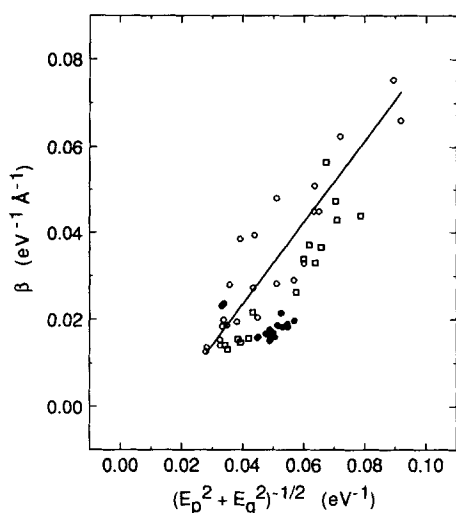


**Figure 10.** Values of  $\beta$  found from the fits of Eqn (3) to the calculated IMFPs plotted versus  $(E_p^2 + E_g^2)^{-1/2}$  for elements ( $\circ$ ), organic compounds ( $\bullet$ ) and inorganic compounds ( $\square$ ). The solid line is a plot of Eqn (4a) with  $\rho = 10 \text{ g cm}^{-3}$ .

this expression is

$$\beta_r = -0.0216 + 7.39 \times 10^{-4} \rho \quad (6)$$

It is clear from Fig. 11 that the group of points for the low-density organic compounds is located below the dashed lines. From a log-log plot of the values of  $\beta_r$  from Eqn (5) vs. density for the elements and the organic compounds, we found that the following expression provided a satisfactory fit to the data

$$\beta_r = -0.10 + 0.069 \rho^{0.1} \quad (7)$$

Equation (7) is shown as the solid line in Fig. 11.

Our modified expression for the parameter  $\beta$  is then

$$\beta_M = -0.10 + 0.944(E_p^2 + E_g^2)^{-1/2} + 0.069 \rho^{0.1} \quad (8)$$

Figure 12 shows plots of values of  $\beta$  from Eqn (4a) and  $\beta_M$  from Eqn (8) vs.  $\beta_{\text{obs}}$ , where  $\beta_{\text{obs}}$  represents values of  $\beta$  determined from the fits of Eqn (3) to the calculated IMFPs for the groups of elements, organic

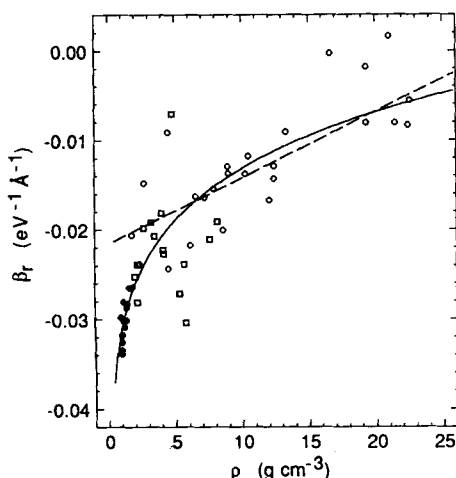


**Figure 11.** Plot of  $\beta_r$  defined by Eqn (5) as a function of density for elements ( $\circ$ ), organic compounds ( $\bullet$ ) and inorganic compounds ( $\square$ ). The dashed line is a plot of Eqn (6) and the solid line shows Eqn (7).

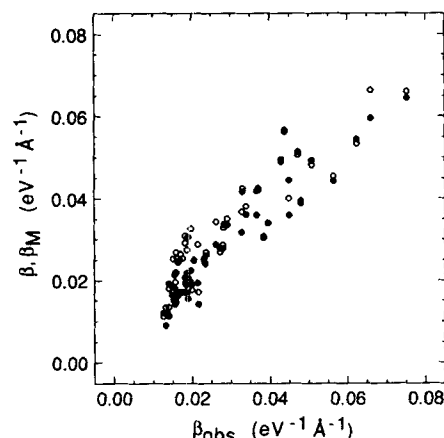


**Figure 12.** Plot of values of  $\beta$  from Eqn (4a) ( $\circ$ ) and values of  $\beta_M$  from Eqn (8) ( $\bullet$ ) vs.  $\beta_{\text{obs}}$ , where  $\beta_{\text{obs}}$  represents values of  $\beta$  determined from the fits of Eqn (3) to the calculated IMFPs for the groups of elements, organic compounds and inorganic compounds.

compounds and inorganic compounds. Each value of  $\beta_{\text{obs}}$  corresponds to a particular material for which there are corresponding values of  $\beta$  and  $\beta_M$  determined from Eqns (4a) and (8), respectively. As the value of  $\beta$  (or  $\beta_M$ ) directly affects the magnitude of computed IMFPs, we show in Fig. 13 the percentage difference between  $\beta$  and  $\beta_M$  as a function of  $\beta$  for the materials in our three groups. The group of points for the organic compounds (solid circles in Fig. 13) shows an average difference of  $\sim 35\%$  between the values of  $\beta$  and  $\beta_M$ . For most of the elements and inorganic compounds, the differences between  $\beta$  and  $\beta_M$  are fairly small (less than  $\pm 10\%$ ). There are, however, four elements for which the differences are greater than or equal to  $10\%$ : Al (10%), C (30%), Mg (10%) and Si (14%). There are eight inorganic materials with differences greater than  $10\%$ :  $\text{Al}_2\text{O}_3$  (15%), KCl (14%), LiF (32%), NaCl (16%), SiC (16%),  $\text{Si}_3\text{N}_4$  (15%),  $\text{SiO}_2$  (27%) and ZnS (11%). For each of these elements and inorganic compounds and for all of the organic compounds,  $\beta_M$  is less than  $\beta$  and, as a result, computed IMFPs from Eqns (3) and (8) will be

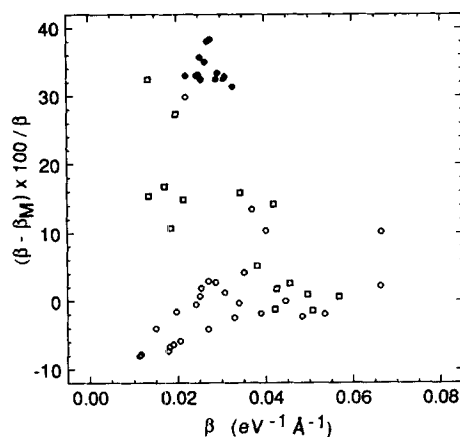


**Figure 13.** Values of the percentage difference in  $\beta_M$  from  $\beta$  as a function of  $\beta$  for elements ( $\circ$ ), organic compounds ( $\bullet$ ) and inorganic compounds ( $\square$ ).

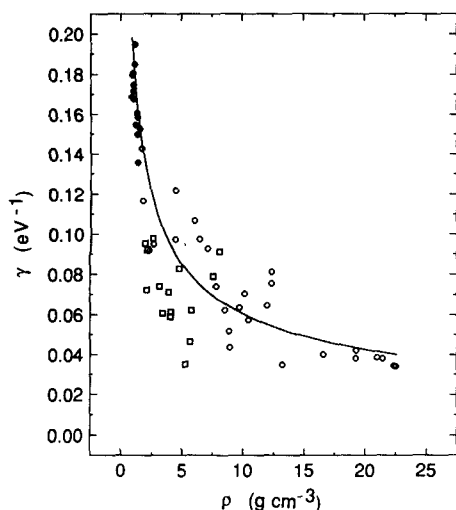
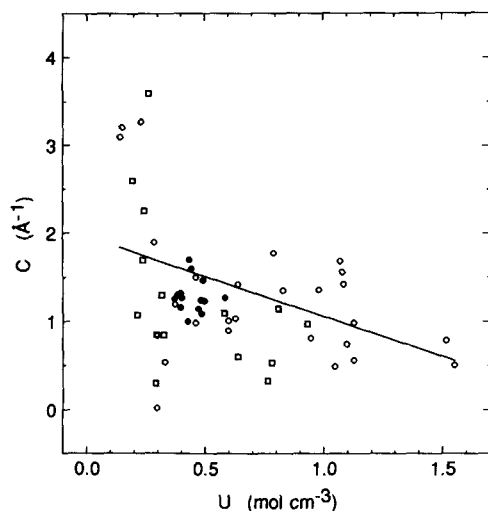


**Figure 14.** Values of  $\gamma$  found from the fits of Eqn (3) to the calculated IMFPs vs. density for elements ( $\circ$ ), organic compounds ( $\bullet$ ) and inorganic compounds ( $\square$ ). The solid line is a plot of Eqn (4b).

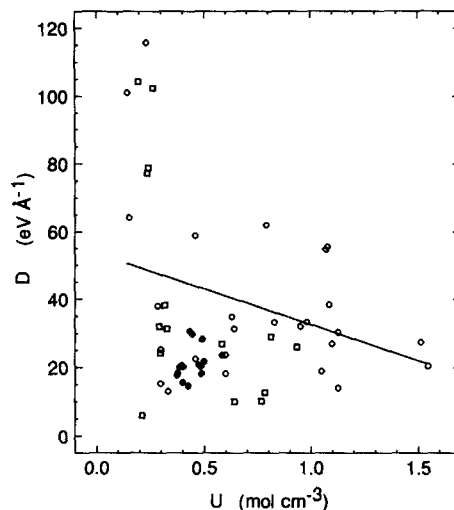
larger than with IMFPs computed from Eqns (3) and (4a).

Figure 14 shows values of  $\gamma$  determined from the fits of Eqn (3) to the calculated IMFPs for each material vs. density. The values of  $\gamma$  for the organic compounds (solid circles) do not differ significantly from Eqn (4b), the solid line, even though Eqn (4b) was obtained from the analysis of elemental solids with generally much higher density than the organic compounds.

Figures 15 and 16b show plots of the values of  $C$  and  $D$  for each material vs.  $U$ . The values of  $C$  for the organic compounds (solid circles in Fig. 15) lie reasonably close to the solid line representing Eqn (4c). In contrast, the values of  $D$  for the organic compounds (solid circles in Fig. 26) fall substantially below the solid line [Eqn (4d)], although these points lie within the appreciable scatter of points for the elements and inorganic compounds.



**Figure 15.** Values of  $C$  found from the fits of Eqn (3) to the calculated IMFPs vs.  $U$  [Eqn (4e)] for elements ( $\circ$ ), organic compounds ( $\bullet$ ) and inorganic compounds ( $\square$ ). The solid line is a plot of Eqn (4c).



**Figure 16.** Values of  $D$  found from the fits of Eqn (3) to the calculated IMFPs vs.  $U$  [Eqn (4e)] for elements ( $\circ$ ), organic compounds ( $\bullet$ ) and inorganic compounds ( $\square$ ). The solid line is a plot of Eqn (4d).

Equations (3), 4(b), 4(c), 4(d), 4(e) and (8) constitute our modified predictive IMFP equation TPP-2M. The only difference between TPP-2M and TPP-2 is that Eqn (8) is used to obtain values of the parameter  $\beta$  instead of Eqn (4a).

Figures 4–8 show evaluations of TPP-2M for five members of our group of organic solids. It can be seen that IMFPs from TPP-2M agree much better with the IMFPs calculated from the optical data than the values obtained from TPP-2.

Figure 17 shows plots of the ratios of IMFPs calculated from TPP-2M to IMFPs calculated from the optical data. Ideally, these ratios should not change with energy and should be close to unity. The ratios are reasonably constant with energy for energies above 200 eV, but there are larger variations for lower energies, particularly below 100 eV. The degree of scatter of the points in Fig. 17 illustrate the success to which TPP-2M

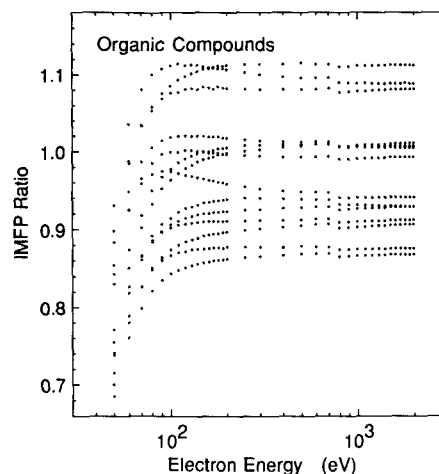


**Figure 17.** Ratios of IMFPs calculated from TPP-2M to IMFPs calculated from optical data (Table 3) as a function of electron energy for the group of organic compounds. The small discontinuity visible between 700 and 800 eV is due to the use of two methods for the IMFP calculations for  $E \leq 700$  eV and  $E \geq 800$  eV (see text).



**Table 6.** Root-mean-square (RMS) deviations between IMFP values from TPP-2M and those calculated from optical data (Table 3) for the group of organic compounds

Compound	RMS deviation (%)
26- <i>n</i> -Paraffin	5.5
Adenine	3.0
$\beta$ -Carotene	13.7
BPA	4.8
DNA	8.8
Diphenyl-hexatriene	15.2
Guanine	9.7
Kapton	5.4
Polyacetylene	10.5
Poly(butene-1-sulfone)	3.2
Polyethylene	7.9
PMMA	10.4
Polystyrene	9.5
Poly(2-vinylpyridine)	12.1

represents the IMFP dependences on material parameters.

Table 6 gives a listing of the RMS deviation for each organic compound in comparison of IMFP values from TPP-2M and those calculated from the optical data (Table 3). The average RMS deviation for the organic compounds is 8.5%; this value is comparable to the uncertainties of the optical data (Table 2) and is considered acceptably small given the empirical nature of TPP-2M.

We have investigated whether TPP-2M satisfactorily describes IMFPs for our groups of elements and inorganic compounds. Tables 7 and 8 show similar listings of the RMS deviations between IMFPs from TPP-2M and those calculated from the optical data. The average RMS deviation for the elements is 10.2%, and this is also considered to be acceptably small based on the errors in the optical data.<sup>1</sup> The largest RMS deviation in the previous comparison with TPP-2 was for carbon (33%).<sup>2</sup> At the time of this analysis, the reason for this large deviation was not known. The corresponding deviation with TPP-2M is now  $\sim 2\%$ ; it is now realized that the original large deviation with TPP-2 and the reduction with TPP-2M is associated with the low density of carbon. Large RMS deviations are seen in Table 7 for Al (23%), Pd (20%) and Re (22%); the reasons for these deviations are possibly associated with errors in the optical data<sup>1</sup> and the empirical nature of TPP-2M.

The RMS deviations for the inorganic compounds in Table 8 are much larger than those found with the groups of elements and organic compounds. We have previously shown that these large deviations are associated with limitations of the optical data (as revealed by our sum-rule tests).<sup>3</sup> We previously<sup>3</sup> recommended using TPP-2 for calculating IMFPs in these compounds, but now recommend the use of TPP-2M.

Table 9 contains a comparison of the average RMS deviations in comparisons of IMFPs from TPP-2 and TPP-2M with IMFPs calculated from optical data for the groups of elements, organic compounds and inorganic compounds. While the improvement of TPP-2M

**Table 7.** Root-mean-square (RMS) deviations between IMFP values from TPP-2M for the group of elements and the IMFPs calculated from optical data<sup>2</sup>

Element	RMS deviation (%)
C	1.7
Mg	8.7
Al	22.7
Si	2.3
Ti	5.6
V	8.6
Cr	6.1
Fe	1.7
Ni	9.3
Cu	14.2
Y	16.8
Zr	10.5
Nb	16.2
Mo	3.5
Ru	4.4
Rh	2.6
Pd	20.1
Ag	10.3
Hf	6.3
Ta	17.4
W	14.9
Re	21.7
Os	4.1
Ir	11.6
Pt	8.6
Au	13.0
Bi	13.1

over TPP-2 is marginal for the group of elements, there is a substantial improvement for the group of organic compounds. As just noted, the RMS deviations for the inorganic compounds are largely associated with uncer-

**Table 8.** Root-mean-square (RMS) deviations between IMFP values from TPP-2M for the group of inorganic compounds and the IMFPs calculated from optical data<sup>3</sup>

Compound	RMS deviation (%)
Al <sub>2</sub> O <sub>3</sub>	15.3
GaAs	39.6
GaP	16.4
InAs	29.2
InP	20.6
InSb	31.5
KCl	9.1
LiF	49.2
NaCl	22.8
PbS	8.2
PbTe	6.3
SiC	3.2
Si <sub>3</sub> N <sub>4</sub>	11.8
SiO <sub>2</sub>	3.6
ZnS	16.5

**Table 9. Summary of the average RMS deviations in comparisons of IMFPs from the predictive formulae TPP-2 and TPP-2M with IMFPs calculated from optical data for the groups of elements, organic compounds and inorganic compounds**

Material group	Average RMS error (%)	
	TPP-2	TPP-2M
Elements	11.6	10.2
Organic compounds	39.0	8.5
Inorganic compounds	21.0	18.9

tainties in the IMFPs from the optical data due to limitations of the optical data.<sup>3</sup> Other comments on the sources of uncertainty in the use of predictive equations such as TPP-2 and TPP-2M are given in Paper IV of this series.<sup>4</sup> We note finally that the largest deviations between IMFPs from TPP-2M and those calculated from optical data occur for electron energies below 200 eV.<sup>4</sup>

We conclude this section by noting that we have also evaluated a possible simplification in TPP-2M. As there is a large scatter of the points about the lines in Figs 15 and 16, we considered whether constant values of the parameters  $C$  and  $D$  (i.e. independent of  $U$ ) would yield satisfactory results. We selected the following average values,  $C = 1.30$  and  $D = 32.6$ , based on the fits of Eqn (3) to the IMFPs calculated for the groups of elements and organic compounds. The averages of the RMS deviations between the IMFPs from this simplified version of TPP-2M and the IMFPs calculated from the optical data were found to be 18.4%, 9.3% and 21.2% for the groups of elements, organic compounds, and inorganic compounds, respectively. These deviations are greater than the corresponding deviations for TPP-2M in Table 9, and we conclude that our proposed simplification is undesirable. While the deviations of the points about the lines in Figs 14 and 15 are substantial, the scatter is due to correlations in the values of  $C$  and  $D$  found in the fits of Eqn (3) to the IMFPs calculated from the optical data.<sup>2</sup> We conclude that the dependences of  $C$  and  $D$  on  $U$  [Eqns (4c) and (4d)] is desirable for TPP-2M.

## DISCUSSION

Ashley<sup>23</sup> has developed a simple expression for the IMFP due to valence-electron excitations,  $\lambda_v$ , in condensed organic materials. He has analyzed values of the energy loss function for 12 of the 14 organic solids considered here and for glycerol. As the energy loss functions for the organic compounds are very similar in shape (cf. Fig. 1), Ashley approximated the main peak in each case with a single Drude-type function. He was then able to apply a 'one-mode' approximation for  $\epsilon(\omega, q)$  and to calculate  $\lambda_v$  for each material; a feature of this work was an estimate of the efforts of electron exchange.

Ashley<sup>23</sup> reported numerical  $\lambda_v$  results only for polyethylene. His values exceed those for polyethylene in Table 3 by 8–17% for energies between 150 and 2000

eV. Ashley's  $\lambda_v$  values are expected to be systematically greater than the present IMFP results because the contributions of core-electron excitations have been included in our IMFP calculations; the contribution of core-electron excitations is typically less than ~10% of the valence-electron contribution to the IMFP. In later work, Ashley<sup>25</sup> reported revised IMFPs for polyethylene that were based on optical data; the newer IMFPs are 10–22% larger than our IMFPs for the 150–2000 eV energy range.

Ashley<sup>23</sup> proposed the following equation based on his  $\lambda_v$  results for estimating  $\lambda_v$  values in other organic materials when the shape of the energy loss function is not known

$$\lambda_v U = E/[14.1 \ln E - 25.5 - (1500/E)] \quad (9)$$

Equation (8) is expected to be useful for electron energies greater than ~150 eV. The corresponding form of Eqn (3) is

$$\lambda U = E/\{829.4[\beta \ln(\gamma E) - (C/E) + (D/E^2)]\} \quad (10)$$

where both  $\lambda_v$  and  $\lambda$  have been expressed in angstroms,  $E$  has been expressed in electron-volts and  $U$  is given by Eqn (4e).

Figure 18 shows a plot of Eqn (9) (solid line) and values of  $\lambda U$  based on the IMFP results in Table 3 for our group of organic compounds. As expected,  $\lambda_v U$  values at any energy are larger than the median of values of  $\lambda U$  from our data because of the effect of core-electron excitations. We also note that the range of  $\lambda U$  values at any energy varies from 1.47 to 1.60, while the range of IMFP values (Table 3 and Fig. 9) at any energy varies from 1.38 to 1.47. While Eqn (9) is only intended as an approximate guide, we see that its use does not reduce the IMFP range amongst the materials in Table 3. The additional material-dependent terms in Eqn (10) provide a satisfactory representation of our IMFP results over the 50–2000 eV range for our groups of elements, organic compounds and inorganic compounds, as indicated by the results for TPP-2M in Table 9.

Ashley<sup>26</sup> has also reported IMFP calculations for poly(butene-1-sulfone) based on a model in which

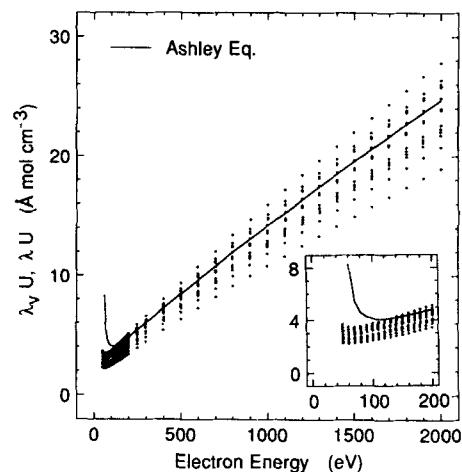


**Figure 18.** Plot of  $\lambda_v U$  (the Ashley equation) from Eqn (9) (solid line) as a function of electron energy. Values of  $\lambda U$  (●) are for the group of organic compounds [IMFP values from Table 3 and  $U$  values from Eqn (4e)]. The inset shows the low-energy region on an expanded energy scale.

optical absorption data for this compound were fitted to a model function appropriate for an insulator. We have utilized the same optical data in our IMFP calculations and obtain very similar IMFPs (within 8%) to those reported by Ashley for electron energies greater than 200 eV; at 50 eV, however, the difference is ~30% due to a correction for electron exchange included by Ashley.

Seah and Dench<sup>27</sup> have analyzed separately electron attenuation length<sup>28</sup> (AL) data for groups of elements, inorganic compounds and organic compounds. The number of AL measurements at the time of their analysis was very limited but, based on the trends found for the other two groups of materials, Seah and Dench proposed the following relationship for describing the AL dependence on electron energy for the organic compounds:

$$\lambda_d = 49E^{-2} + 0.11E^{1/2} \text{ mg m}^{-2} \quad (11)$$

The solid line in Fig. 19 shows a plot of Eqn (11). The solid circles in Fig. 19 indicate the IMFP results for our group of organic compounds expressed in mass-thickness units (i.e.  $\lambda_d = \rho\lambda_A/10$ , where  $\lambda_A$  is the IMFP in angstrom units). While there is a rough correspondence in the values of  $\lambda_d$  from Eqn (11) and our IMFP data, we see that there are appreciable differences, particularly for energies less than ~500 eV. The range in  $\lambda_d$  values obtained from our IMFPs at a given energy varies from 1.49 to 1.64; this spread is similar to that shown in Fig. 18, and is larger than the spread of IMFP values in Table 3. We also note that Eqn (11) indicates that the minimum value of  $\lambda_d$  occurs at an energy of ~20 eV, whereas the minimum values of our calculated IMFPs occur at 60–70 eV.

Ashley<sup>23</sup> pointed out in 1982 that experimental AL values for organic compounds show considerable variation; possible reasons for such scatter have been discussed elsewhere.<sup>28,29</sup> Several AL measurements in organic compounds have been reported more recently.<sup>30–32</sup> Kurtz *et al.*<sup>30</sup> find ALs of ~10 Å and ~9 Å for 18–64 eV electrons in condensed methanol and cyclohexane, respectively, and only a slight dependence on energy in this range; these values were larger than

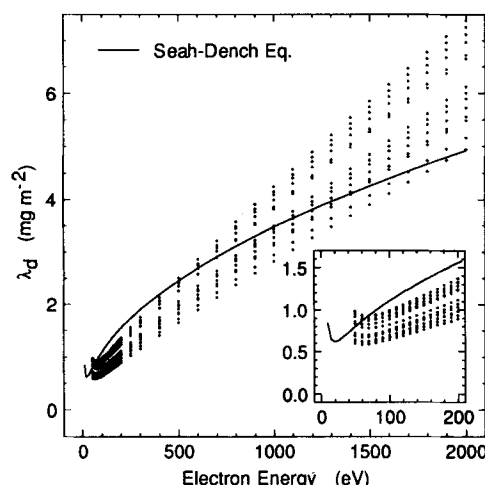


**Figure 19.** Plot of the Seah and Dench expression (solid line) for organic compounds from Eqn (11). Values of  $\lambda_d$  (●) are calculated from our IMFP values (Table 3). The inset shows the low-energy region on an expanded energy scale.

expected from the Seah–Dench equation [Eqn (11)] but are consistent with the trends of the calculated IMFPs in Fig. 19. Cartier *et al.*<sup>31</sup> reported ALs for 0.1–4500 eV electrons in hexatriacontane ( $C_{36}H_{74}$ ); their values in the 50–200 eV range are up to about twice the IMFPs for 50–200 eV electrons in 26-*n*-paraffin (Table 3), but for 500–2000 eV electrons their ALs are about 50% larger than the corresponding IMFPs for 26-*n*-paraffin. Finally, Sastry *et al.*<sup>32</sup> measured ALs for 550–1350 eV electrons in lead arichidate  $[(C_{19}H_{39}COO)_2Pb]$  Langmuir–Blodgett films. They pointed out that their ALs were substantially greater than IMFPs computed from TPP-2. The use of TPP-2M reduces the differences, but the measured ALs are still about 40–80% larger than the computed IMFPs.

We have previously<sup>4</sup> compared our computed IMFPs with the equation proposed by Wagner *et al.*<sup>33</sup> for describing the dependence of measured ALs on electron energy

$$\lambda_{AL} = kE^m \quad (12)$$

where  $\lambda_{AL}$  is the AL (in Å) and  $k$  and  $m$  are parameters. We found that satisfactory fits of Eqn (12) to the calculated IMFPs for the groups of elements and inorganic compounds could be obtained over the 500–2000 eV range and that the average value of the exponent  $m$  was 0.75 for these materials.<sup>4</sup> Figure 20 shows a fit of Eqn (7) to the calculated IMFPs for polystyrene as an example for our organic compounds. Table 10 shows values of the parameters  $k$  and  $m$  resulting from our fits. The values of  $k$  range from 0.107 to 0.149 Å, while the values of  $m$  vary between 0.781 and 0.795. The average value of  $m$  for the organic compounds (0.79) is thus slightly larger than the corresponding values for the groups of elements and inorganic compounds (0.75); this difference is associated with the different average densities for these groups of compounds.

We found previously<sup>4</sup> that the modified Bethe equation [Eqn (3)] provides a much better fit to the calculated IMFPs for the groups of elements and inorganic compounds than Eqn (12). Figure 20 shows, as an

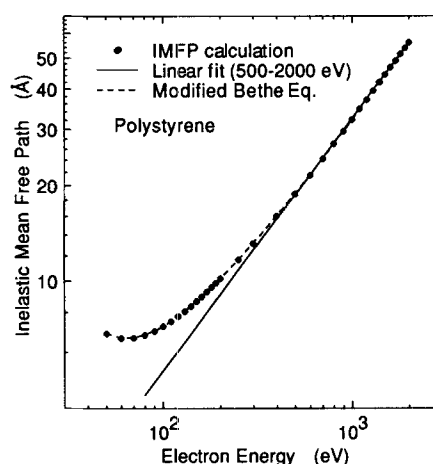


**Figure 20.** Plot of calculated IMFPs for polystyrene (●) as a function of electron energy on logarithmic scales. The solid line is a fit of Eqn (12) to the calculated IMFPs over the 500–2000 eV range. The dashed line is a fit of the modified Bethe equation [Eqn (3)] to the calculated IMFPs over the 50–2000 eV range with the four parameters  $\beta$ ,  $\gamma$ ,  $C$  and  $D$  allowed to vary; the values of these parameters resulting from the fit are listed in Table 4.

**Table 10.** Values of the parameters  $k$  and  $m$  in the fits of Eqn (12) to the calculated IMFPs for the group of 14 organic compounds (Table 3) over the electron energy range 500–2000 eV

Compound	$k$ (Å)	$m$
26- <i>n</i> -Paraffin	0.145	0.794
Adenine	0.125	0.787
$\beta$ -Carotene	0.133	0.795
BPA	0.132	0.790
DNA	0.130	0.792
Diphenyl-hexatriene	0.132	0.794
Guanine	0.116	0.784
Kapton	0.128	0.781
Polyacetylene	0.107	0.790
Poly(butene-1-sulfone)	0.139	0.782
Polyethylene	0.137	0.790
PMMA	0.149	0.786
Polystyrene	0.138	0.790
Poly(2-vinylpyridine)	0.138	0.791

example, the superiority of Eqn (3) in fitting IMFPs for polystyrene. Jablonski<sup>34</sup> has also pointed out the advantages of the Bethe equation [i.e. Eqn (3) without the last two terms] over Eqn (12).

## SUMMARY

We have calculated IMFPs from experimental optical data for 50–2000 eV electrons in 14 organic compounds. This group of compounds had very similar electron energy loss functions and, as a result, the computed IMFPs were of similar magnitude and showed similar dependences on electron energy.

We compared our calculated IMFPs for the organic compounds with values predicted by the TPP-2 formula that we developed earlier<sup>2</sup> and found differences of ~40%. These differences were traced to the fact that the TPP-2 formula had been developed from IMFPs for a group of high-density elements (generally transition metals) and that the TPP-2 formula was being extrapolated to a group of low-density materials (the organic compounds) for which it had not been previously tested and validated.

We analyzed the IMFPs for the groups of elements and organic compounds together and derived a modified expression for one of the parameters ( $\beta$ ). Our modified predictive IMFP equation TPP-2M [comprising Eqns (2), 4(b), 4(c), 4(d), 4(e) and (8)] gives IMFPs that agree reasonably with the values calculated from the optical data. The RMS deviations between IMFPs from TPP-2M and those calculated from optical data are 10.2% and 8.5% for the groups of elements and organic compounds, respectively; these RMS deviations are considered acceptably small given the uncertainties of the optical data and the empirical nature of TPP-2M. We also recommend TPP-2M over TPP-2 for calculation of IMFPs in inorganic compounds; for these materials, uncertainties in the optical data led to substantial uncertainties in the directly computed IMFPs.<sup>3</sup>

We compared our IMFPs for the organic compounds with a simple IMFP expression proposed by Ashley.<sup>23</sup> This comparison showed that the Ashley expression does not adequately describe the IMFP dependence on material parameters. We also compared our IMFPs to the empirical equation proposed by Seah and Dench<sup>27</sup> for electron attenuation lengths in organic compounds. This AL equation gives a different dependence on electron energy than we find for the IMFPs. In addition, the Seah–Dench equation does not represent adequately the IMFP dependence on material parameters.

## REFERENCES

1. S. Tanuma, C. J. Powell and D. R. Penn, *Surf. Interface Anal.* **11**, 577 (1988), Paper I in this series.
2. S. Tanuma, C. J. Powell and D. R. Penn, *Surf. Interface Anal.* **17**, 911 (1991), Paper II in this series.
3. S. Tanuma, C. J. Powell and D. R. Penn, *Surf. Interface Anal.* **17**, 927 (1991), Paper III in this series.
4. S. Tanuma, C. J. Powell and D. R. Penn, *Surf. Interface Anal.* **20**, 77 (1993), Paper IV in this series.
5. H. Bethe, *Ann. Phys.* **5**, 325 (1930).
6. D. R. Penn, *Phys. Rev. B* **35**, 482 (1987).
7. T. Okabe, *J. Phys. Soc. Jpn* **35**, 1496 (1973).
8. B. L. Henke, J. C. Davis, E. M. Gullikson and R. C. C. Perera, Lawrence Berkeley Laboratory Report 26259 (1988).
9. E. T. Arakawa, L. C. Emerson, S. I. Juan, J. C. Ashley and M. W. Williams, *Photochem. Photobiol.* **44**, 349 (1986).
10. T. Inagaki, R. N. Hamm, E. T. Arakawa and R. D. Birkhoff, *Biopolymers* **14**, 839 (1975).
11. T. Inagaki, R. N. Hamm, E. T. Arakawa and L. R. Painter, *J. Chem. Phys.* **61**, 4246 (1974).
12. L. C. Emerson, M. W. Williams, I'an Tang, R. N. Hamm and E. T. Arakawa, *Radiat. Res.* **63**, 235 (1975).
13. E. T. Arakawa, M. W. Williams, J. C. Ashley and L. R. Painter, *J. Appl. Phys.* **52**, 3579 (1981).
14. J. J. Ritsko, *Phys. Rev. B* **26**, 2192 (1982).
15. M. W. Williams, D. W. Young, J. C. Ashley and E. T. Arakawa, *J. Appl. Phys.* **58**, 4360 (1985).
16. L. R. Painter, E. T. Arakawa, M. W. Williams and J. C. Ashley, *Radiat. Res.* **83**, 1 (1980).
17. J. J. Ritsko, L. J. Brillson, R. W. Bigelow and T. J. Fabish, *J. Chem. Phys.* **69**, 3931 (1978).
18. T. Inagaki, E. T. Arakawa, R. N. Hamm and M. W. Williams, *Phys. Rev. B* **15**, 3243 (1977).
19. J. J. Ritsko and R. W. Bigelow, *J. Chem. Phys.* **69**, 4162 (1978).
20. S. Tanuma, C. J. Powell and D. R. Penn, *J. Electron Spectrosc.* **62**, 95 (1993).
21. M. Inokuti, *Rev. Mod. Phys.* **43**, 297 (1971).
22. J. C. Ashley, *J. Electron Spectrosc.* **46**, 199 (1988).
23. J. C. Ashley, *J. Electron Spectrosc.* **28**, 177 (1982).
24. C. J. Powell, *Surf. Interface Anal.* **10**, 349 (1987); *Ultramicroscopy* **28**, 24 (1989).
25. J. C. Ashley, *J. Electron Spectrosc.* **50**, 323 (1990).
26. J. C. Ashley, *J. Appl. Phys.* **63**, 4620 (1988).
27. M. P. Seah and W. A. Dench, *Surf. Interface Anal.* **1**, 2 (1979).
28. C. J. Powell, *J. Electron Spectrosc.* **47**, 197 (1988).
29. C. Brundle, H. Hopster and J. D. Swalen, *J. Chem. Phys.* **70**, 5190 (1979).
30. R. L. Kurtz, N. Usuki, R. Stockbauer and T. E. Madey, *J. Electron Spectrosc.* **40**, 35 (1986).
31. E. Cartier, P. Pfluger, J.-J. Pireaux and M. Rei Vilar, *Appl. Phys. A* **44**, 43 (1987).
32. M. Sastry, S. Badrinarayanan and P. Ganguly, *Phys. Rev. B* **45**, 9320 (1992).
33. C. D. Wagner, L. E. Davis and W. M. Riggs, *Surf. Interface Anal.* **2**, 53 (1980).
34. A. Jablonski, *Surf. Interface Anal.* **20**, 317 (1993).